



OPEN

Electrochemically induced Meerwein arylation as a green strategy for the synthesis of arylbenzoquinone derivatives under batch and flow conditions

Mozhdeh Malmir¹, Davood Nematollahi^{1,2✉}, Ali Sadatnabi¹ & Sajad Shanehsaz¹

An electrochemical Meerwein arylation reaction was reported for the synthesis of aryl-benzoquinone derivatives. In this work, efficient electrochemical synthesis of aryl-benzoquinone derivatives by direct electrolysis of aqueous solution containing hydroquinone and aryldiazonium salts in batch and a homemade continuous-flow cells is reported. In the batch system, the products were obtained in a simple undivided cell equipped with a copper anode and a stainless steel cathode. In the continuous flow system, the products were obtained simply by passing hydroquinone and the aryldiazonium salt through a tube made of copper with a stainless steel rod in the center. All equipment required in both cell types is obtained from common commercial sources. This protocol is green and cost-effective due to the use of electricity and is performed under mild and safe conditions without the use of toxic solvents and catalysts.

Keywords Aryldiazonium salt, Continuous-flow cell, Copper anode, Cyclic voltammetry, Hydroquinone

Electrochemistry is a very efficient tool for the synthesis of organic compounds, which has recently attracted the attention of many researchers^{1–14}. It has been found that in many cases, electrochemical synthesis can be a suitable alternative to chemical synthesis. From another point of view, electrochemical synthesis of organic compounds is well established as an environmentally friendly strategy. Benzoquinones are a group of organic compounds that are involved in important biological activities such as electron transport processes, oxidative phosphorylation and bioenergetic transport. In addition, some of them have anti-cancer, anti-inflammatory and antioxidant activities¹⁵. Therefore, the synthesis of these compounds can be useful in the development of some medicinal molecules. Among quinones, *p*-benzoquinones are the simplest members of quinones, which are used in the manufacture of dyes and fungicides. They are also important organic intermediates in the synthesis of pharmaceuticals and fine chemicals¹⁶. Literature review shows that many researchers have synthesized *p*-benzoquinones in different routes^{17–27}. Moore and co-workers reported the synthesis of 1,4-benzoquinones from 4-alkynyl-4-alkoxy (or hydroxy or trimethylsilyloxy) cyclobutenones¹⁷. The reaction is performed through electrocyclic ring opening of cyclobutenones to (2-alkynylethenyl)ketenes, then ring closing and diradical formation. George et al. reported the synthesis of 2-substituted 1,4-benzoquinones via oxidative dearomatization of *para*-substituted phenols using singlet oxygen in supercritical CO₂¹⁸. The synthesis was carried out in a continuous multi-step in supercritical CO₂. Saa et al. reported an oxidative degradation method by Fremy's salt for the synthesis of quinones¹⁹. They performed these syntheses using phenols that have both a coordinating group for chelation and an electron withdrawing group in a 1,3-relationship. In 2008, Mathur and co-workers reported the photochemical synthesis of the 2,6- and 2,5-divinyl-substituted 1,4-benzoquinones from the reaction of enynes, (*Z*)-1-methoxybut-1-ene-3-yne, or isopropenyl acetylene with CO in the presence of Fe(CO)₅²⁰. In 2019, Kim et al. reported the synthesis of benzoquinones from hydroquinones using an activated carbon-molecular oxygen system²¹. In this method, the synthesis of benzoquinone was carried out via the oxidation of hydroquinone by oxygen (1 atm) in xylene (0.1 M) at 120 °C for 24 h. These methods have disadvantages due to the use of highly corrosive and expensive oxidants and solvents. Therefore, some researchers

¹Faculty of Chemistry and Petroleum Sciences, Bu-Ali Sina University, Hamedan 65178-38683, Iran.

²Planet Chemistry Research Center, Bu-Ali Sina University, Hamedan, Iran. ✉email: nemat@basu.ac.ir; dnematollahi@yahoo.com

have used electrochemical methods for the synthesis of 1,4-benzoquinones. In 2022, Waldvogel and co-workers reported the electrochemical synthesis of *para*-benzoquinones from phenols using a continuous flow cell in a water/methanol mixture without the use of a catalyst and chemical oxidizer with 61–99% yield²². Nematollahi et al. synthesized a number of mono- and di-substituted *p*-benzoquinone electrochemically through the oxidation of hydroquinone at carbon anode in the presence of some nucleophiles in a water/acetonitrile mixture^{23,24}. Raju and co-workers reported the electrochemical synthesis of *p*-benzoquinones in biphasic medium (water/dichloromethane) from 1,4-dihydroxy benzenes using platinum foil electrodes²⁵. In 2023, Zhang et al. reported the synthesis of *p*-benzoquinones (in moderate to good yields) from the electrochemical oxidation of simple aromatic compounds²⁶. Electrolysis was carried out in CH₃CN/H₂O (5/1) containing *n*Bu₄NBF₄ (0.1 M) and K₂S₂O₈ using platinum electrodes applying a constant current of 10 mA at room temperature. Recently, Waldvogel et al. synthesized a number of *p*-benzoquinones (up to 99% yield) electrochemically in water/methanol mixture through the oxidation of 4-hydroxybenzaldehydes using a graphite anode²⁷.

Meerwein arylation²⁸ is one of the most widely used methods for the functionalization of alkenes through radical reactions. In this method, the first step is usually the generation of aryl radicals from various precursors and with different methods²⁹. The next step in this method is the reaction of the aryl radical with an alkene and the formation of a radical adduct. In the last step, depending on the conditions, this radical adduct after reduction can react with the electrophile and produces the final product. Or after oxidation, reacts with a nucleophile to form the product or in the presence of a radical scavenger to form the final product (Fig. 1)²⁹. It should be noted that in this method, aryldiazonium salts are often the source of aryl radicals.

A literature survey reveals that the Meerwein method for the arylation of organic compounds has been used in a large number of papers^{29–32}. Despite the large number of articles, to the best of our knowledge there are no reports on electrochemically induced Meerwein arylation. Considering the advantages mentioned for electroorganic synthesis^{1–14}, we decided to perform the Meerwein arylation by electrochemical method. In this work, the electrochemical synthesis of aryl-benzoquinone derivatives from the direct electrolysis of an aqueous solution containing hydroquinone in the presence of aryldiazonium salts in both batch and continuous-flow cells is performed. The proposed method is carried out under mild and safe conditions without the use of toxic solvents and catalysts and is very economical due to the use of electricity.

Experimental

Reagents and apparatus

All syntheses were performed at room temperature by applying a constant current using a Chin PS-303 DC power supply. The solution was stirred with a magnetic stirrer (Rodwell, Monostir, England) during electrolysis. FTIR spectroscopy was used to identify the functional groups of the products. All spectra were recorded from 4000 to 400 cm^{−1} with a KBr disk on a Perkin–Elmer GX FTIR spectrometer. All ¹H NMR and ¹³C NMR were recorded in CDCl₃ on a Bruker Avance DRX 400 spectrometer. The spectrometer operates at 400 MHz for protons and 100 MHz for carbon. The chemical shifts are reported in ppm (δ) at 298 K. All melting points in open capillary tubes were measured using a Model 9100 electrothermal apparatus and are uncorrected. AutoLab/PGSTAT30 potentiostat/galvanostat (manufactured by Eco Chemie, Utrecht, The Netherlands) was used for cyclic voltammetry studies. Constant current electrolysis was performed using a DC POWER SUPPLY PS-305D power supply. The three-electrode system used for cyclic voltammetry measurements consisted of a glassy carbon disc (diameter 1.8 mm) as a working electrode, a stainless steel wire as an auxiliary electrode and Ag/AgCl (3 M) electrode as a reference electrode. All electrodes are provided by Azar Electrode Company (Iran). Alumina slurry was used to polish the glassy carbon electrode. Electrochemical synthesis of aryl-benzoquinone derivatives was performed in both batch and flow cells. The undivided cylindrical batch cell (100 mL) equipped with a large copper plate (5.5 cm × 2.5 cm) as the anode and a stainless steel rod with a length of 4 cm as a counter electrode (cathode). The continuous flow cell consists of a tube made of copper with a length of 28 cm and diameter of 1.3 cm (as the anode) and a stainless steel rod cathode with the same length and diameter of 1.2 cm in the center as the anode.

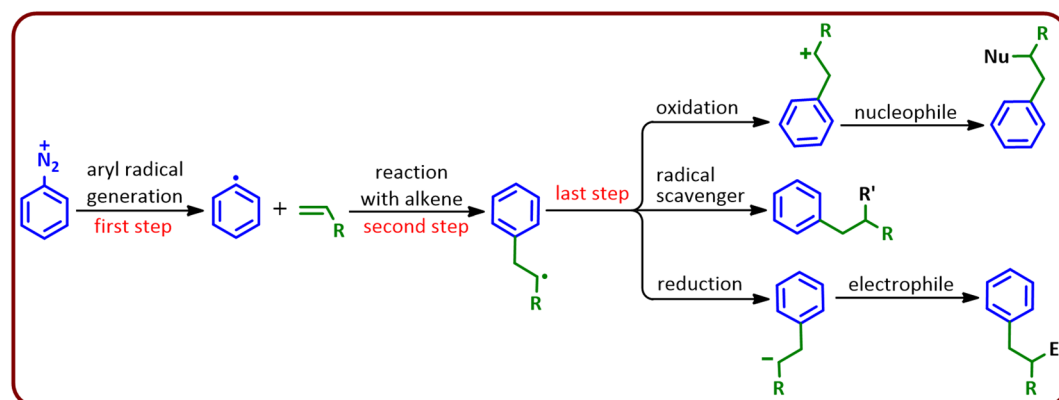


Fig. 1. Reaction pathways in Meerwein arylation.

Chemicals used in this study (aniline, 4-nitroaniline, 4-chloroaniline, 4-bromoaniline, 4-iodoaniline, 4-methoxyaniline, 4-fluoroaniline, hydroquinone and 2-methylhydroquinone) were purchased with purity higher than 98% from Aldrich and Merck. Buffer solutions were prepared according to the recommended procedures³³, from analytical reagent grade chemicals purchased from Merck and Sigma without further purification.

Synthesis of diazonium salt

Sulfuric acid (5 mL) was added to a well-stirred suspension of aniline derivatives (2 mmol) in H₂O (10 mL). The reaction mixture was cooled to 0–5 °C in an ice bath. Then, a cooled solution of sodium nitrite (3 mmol) in H₂O (5 mL) at 0–5 °C was added dropwise to the reaction mixture. At this time, the color of the solution turns yellow, which indicates the formation of diazonium salt. The synthesized diazonium solution (approximate concentration, 0.13 M) is placed in ice bath for use in the next step.

Synthesis of aryl-benzoquinone derivatives in batch cell

For the synthesis of aryl-benzoquinone derivatives, first the aqueous solution of sodium acetate (0.15 M) (80 ml) containing hydroquinone (or 2-methylhydroquinone) (2 mmol) was electrolyzed in an undivided cell equipped with a copper plate anode and a stainless steel rod cathode under constant current (current density = 0.5 mA cm⁻²) (20 mA) for 10 min. After this period, 2 ml of the produced diazonium solution is added to the electrochemical cell. Then electrolysis continues and after every 6 min, 2 ml of diazonium solution is added to the cell, and these steps continue until the diazonium solution is exhausted. The precipitate was collected by filtration and washed several times with distilled water. The dried precipitate was dissolved in acetone and subjected to preparative TLC (silica gel 60 GF 254), *n*-hexane/ethyl acetate 45:15]. The products were isolated as yellow powder. IR, ¹H NMR and ¹³C NMR spectra for new compounds **ABQ8**–**ABQ11** can be obtained in the supplementary material (Figures S1–S20).

Synthesis of aryl-benzoquinone derivatives using undivided tubular flow cell

An undivided tubular flow cell consists of a copper tube as the anode with an inner diameter of 1.3 cm and a length of 28 cm with an area of 114 cm² (Fig. 2). Inside the copper tube is a stainless steel rod with a diameter of 1.0 cm and a length of 28 cm, with an area of 87.9 cm² as a cathode. In this cell, the cathode is surrounded by the anode and the solution is pumped from the bottom of the reactor to the top. The arrangement of anode and cathode is shown in Fig. 2. In order to produce aryl-benzoquinone, a solution of sodium acetate (0.15 M) (80 mL) containing hydroquinone (2 mmol) along with aryl diazonium salt is passed through the flow cell at a constant flow rate using a syringe pump. The cell volume is 15.2 cm³ and the volume of the connecting tubes is 17.5 cm³.

Characteristics of the products

4'-Nitro-[1,1'-biphenyl]-2,5-dione (C₁₂H₇NO₄) (ABQ1). Yellow solid; M.p. 152–154 °C (Lit. 137 °C³⁴); ¹H NMR (400 MHz, DMSO-*d*₆) δ: 8.30 (d, *J* = 8.7 Hz, 2H), 7.79 (d, *J* = 8.7 Hz, 2H), 7.10 (d, *J* = 2.3 Hz, 1H), 7.02 (s, 1H), 6.98 (d, *J* = 2.3 Hz, 1H); IR (KBr) (cm⁻¹): 2924, 2853, 1726, 1664, 1588, 1517, 1462, 1350, 1095, 865, 695; MS (ESI) *m/z* (relative intensity): 231 (M + 2H) (72), 230 (M + 1) (10), 229 (M) (57), 183 (52), 149 (100).

[1,1'-Biphenyl]-2,5-dione (C₁₂H₈O₂) (ABQ2). Yellow solid, M.p. 83–86 °C (Lit. 104–106 °C³⁵); ¹H NMR (400 MHz, CDCl₃) δ: 7.48 (s, 1H), 7.38 (br, 5H), 7.08–6.87 (m, 3H); ¹³C NMR (101 MHz, CDCl₃) δ 187.6, 186.6, 146.5, 137.1, 136.4, 136.3, 132.7, 130.2, 129.2, 128.6; IR (KBr) (cm⁻¹): 2922, 1729, 1654, 1594, 1489, 1227, 1092, 843, 746, 696.

4'-Methoxy-[1,1'-biphenyl]-2,5-dione (C₁₃H₁₀O₃) (ABQ3). Yellow solid, M.p. 108–110 °C (Lit. 108–110 °C³⁶); ¹H NMR (400 MHz, CDCl₃) δ: 7.91 (d, *J* = 8.8 Hz, 2H), 7.50 (s, 1H), 7.03 (d, *J* = 8.8 Hz, 2H), 6.99 (d, *J* = 8.6 Hz, 2H), 3.92 (s, 3H); ¹³C NMR (101 MHz, CDCl₃) δ: 161.1, 158.2, 146.6, 133.0, 127.2, 123.9, 113.8, 55.1; IR (KBr) (cm⁻¹): 2959, 2839, 1601, 1581, 1499, 1465, 1441, 1306, 1251, 1180, 1148, 1042, 1024, 845, 825, 810, 782, 743, 555, 497.

4'-Chloro-[1,1'-biphenyl]-2,5-dione (C₁₂H₇ClO₂) (ABQ4). Yellow solid, M.p. 110–112 °C (Lit. 127–129 °C³⁷); ¹H NMR (400 MHz, CDCl₃) δ: 7.51–7.38 (br, 4H), 6.97–6.77 (br, 3H); ¹³C NMR (101 MHz, CDCl₃) δ: 187.3, 186.3, 144.7, 137.0, 136.6, 136.4, 132.7, 131.0, 130.6, 128.9; IR (KBr) (cm⁻¹): 3069, 1648, 1596, 1492, 1403, 1340, 1305, 1293, 1092, 1016, 976, 904, 855, 842, 822, 790, 728, 564, 508, 470, 419. MS (ESI) *m/z* (relative intensity): 218 (M) (11), 183 (m - Cl) (100), 155 (19), 136 (21), 101 (14), 82 (38).

4'-Bromo-[1,1'-biphenyl]-2,5-dione (C₁₂H₇BrO₂) (ABQ5). Yellow solid; M.p. 84–87 °C (Lit. 100–102 °C³⁸); ¹H NMR (400 MHz, CDCl₃) δ: 7.52 (d, *J* = 8.5 Hz, 2H), 7.29 (d, *J* = 8.6 Hz, 2H), 6.80–6.78 (m, 3H); ¹³C NMR (101 MHz, CDCl₃) δ: 187.3, 186.3, 144.8, 137.0, 136.38, 132.7, 131.8, 130.8, 125.0; IR (KBr) (cm⁻¹): 2926, 1651, 1593, 1489, 1400, 1339, 1292, 1098, 1073, 1012, 978, 906, 852, 789, 709, 501, 425.

4'-Iodo-[1,1'-biphenyl]-2,5-dione (C₁₂H₇IO₂) (ABQ6). Yellow solid; M.p. 127–130 °C (Lit. 133–135 °C³⁹); ¹H NMR (400 MHz, CDCl₃) δ: 7.73 (d, *J* = 8.5 Hz, 2H), 7.15 (d, *J* = 8.5 Hz, 2H), 6.81–6.78 (m, 3H); ¹³C NMR (101 MHz, CDCl₃) δ: 186.3, 185.2, 143.9, 136.7, 136.0, 135.3, 131.6, 130.0, 129.8, 96.0; IR (KBr) (cm⁻¹): 2923, 1647, 1597, 1580, 1483, 1393, 1385, 1342, 1293, 1260, 1097, 1063, 1008, 975, 910, 849, 784, 698, 606, 548, 428.

4'-Fluoro-[1,1'-biphenyl]-2,5-dione (C₁₂H₇FO₂) (ABQ7). M.p. 152–155 °C (Lit. 152–155 °C³⁶); ¹H NMR (400 MHz, CDCl₃) δ: 7.46–7.42 (m, 2H), 7.13–6.79 (m, 5H); IR (KBr) (cm⁻¹): 2924, 1660, 1603, 1508, 1413, 1376, 1330, 1235, 1235, 1162, 1107, 919, 845, 525, 420.

4-Methyl (and 3-methyl)-4'-nitro-[1,1'-biphenyl]-2,5-dione (C₁₃H₉NO₄) (ABQ8, two isomers). M.p. 131–133 °C; ¹H NMR (400 MHz, CDCl₃) δ: 8.25 (d, *J* = 8.7 Hz, 4H), 7.30 (d, *J* = 8.8 Hz, 4H), 6.86 (s, 1H), 6.84 (s, 1H), 6.81 (s, 1H), 6.78 (s, 1H), 2.10 (s, 3H), 2.07 (s, 3H); ¹³C NMR (101 MHz, CDCl₃) δ: 187.2, 186.8, 185.7, 147.9, 146.3, 142.6, 141.9, 139.3, 139.2, 136.7, 136.3, 134.1, 133.7, 133.5, 130.7, 130.3, 130.2, 123.6, 123.5, 16.4, 15.6; IR

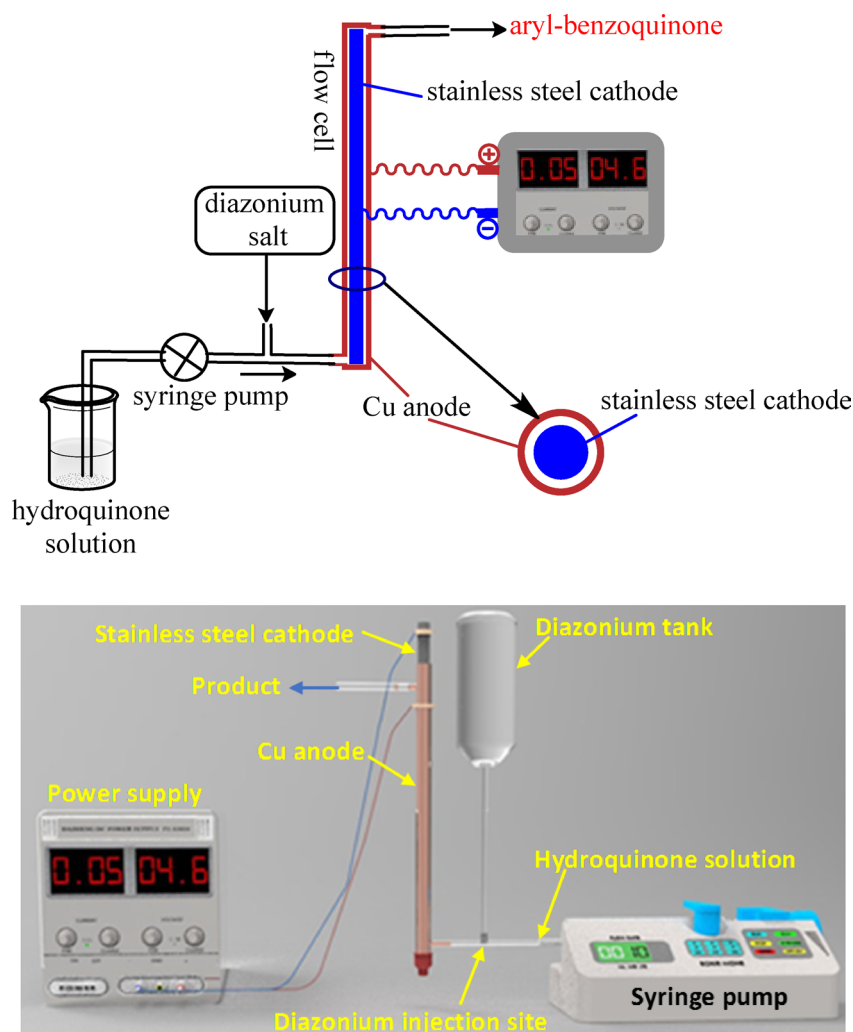


Fig. 2. Schematic diagram (above) and the image (below) of the undivided tubular flow cell for the synthesis of aryl-benzoquinone derivatives.

(KBr) (cm^{-1}): 3114, 3068, 2925, 1656, 1592, 1518, 1348, 1304, 1137, 1091, 946, 865, 846, 749, 699, 410 (Figures S1–S5, Supplementary Material).

4'-Chloro-4-methyl (and 3-methyl) -[1,1'-biphenyl]-2,5-dione ($\text{C}_{13}\text{H}_9\text{ClO}_2$) (**ABQ9**, two isomers); M.p. 64–67 °C; ^1H NMR (400 MHz, CDCl_3) δ : 7.35 (m, 8H), 6.77 (s, 1H), 6.72 (s, 1H), 6.64 (s, 1H), 6.62 (s, 1H), 2.07 (s, 3H), 2.04 (s, 3H); ^{13}C NMR (101 MHz, CDCl_3) δ : 187.8, 187.3, 186.8, 186.5, 146.2, 145.8, 144.9, 144.6, 136.3, 136.2, 133.7, 133.3, 132.74, 132.68, 131.4, 131.0, 130.5, 129.5, 128.8, 128.7, 16.4, 15.5; IR (KBr) (cm^{-1}): 3050, 2974, 1647, 1627, 1594, 1493, 1427, 1404, 1354, 1305, 1231, 1095, 1013, 923, 880, 839, 828, 738, 523, 446, 418 (Figures S6–S10, Supplementary Material).

4'-Bromo-4-methyl (and 3-methyl) -[1,1'-biphenyl]-2,5-dione ($\text{C}_{13}\text{H}_9\text{BrO}_2$) (**ABQ10**, two isomers); M.p. 84–86 °C; ^1H NMR (400 MHz, CDCl_3) δ : 7.60 (d, $J=8.3$ Hz, 4H), 7.38 (d, $J=6.1$ Hz, 4H), 6.87 (s, 1H), 6.81 (s, 1H), 6.73 (s, 1H), 6.71 (s, 1H), 2.16 (s, 3H), 2.13 (s, 3H); ^{13}C NMR (101 MHz, CDCl_3) δ : 187.9, 187.3, 186.5, 186.8, 146.2, 145.9, 144.7, 137.4, 136.5, 136.4, 133.7, 133.3, 132.8, 132.7, 131.8, 131.7, 131.5, 131.2, 130.8, 130.7, 129.8, 124.8, 124.6, 16.4, 15.5; IR (KBr) (cm^{-1}): 2928, 1654, 1630, 1594, 1429, 1398, 1189, 1073, 1010, 917, 828, 458 (Figures S11–S15, Supplementary Material).

4'-Iodo-4-methyl (and 3-methyl) -[1,1'-biphenyl]-2,5-dione ($\text{C}_{13}\text{H}_9\text{IO}_2$) (**ABQ11**, two isomers); ^1H NMR (400 MHz, CDCl_3) δ : 7.71 (d, $J=8.0$ Hz, 4H), 7.14 (d, $J=6.0$ Hz, 4H), 6.77 (s, 1H), 6.71 (s, 1H), 6.64 (s, 1H), 6.62 (s, 1H), 2.06 (s, 3H), 2.0 (s, 3H); ^{13}C NMR (101 MHz, CDCl_3) δ : 187.9, 187.4, 186.7, 186.5, 146.2, 145.9, 145.2, 144.8, 137.73, 137.69, 137.4, 136.5, 136.4, 133.8, 133.3, 132.73, 132.67, 131.3, 130.9, 130.8, 96.8, 16.4, 15.6; IR (KBr) (cm^{-1}): 2922, 1651, 1626, 1599, 1579, 1485, 1396, 1354, 1305, 1231, 1192, 1125, 1061, 1004, 919, 826, 801, 722, 670, 512, 471 (Figures S16–S20, Supplementary Material).

Results and discussion

Electrochemical studies

In order to obtain the detailed information about the reaction between *p*-benzoquinone and aryldiazonium salts, the electrochemical behavior of hydroquinone in the presence of 4-nitrobenzenediazonium sulfate was investigated. Figure 3, part I, curve a, shows the cyclic voltammogram of hydroquinone (HQ) (1 mM) in aqueous acidic/ethanol (50/50 v/v) mixture. It should be noted that to record this voltammogram, 1 ml of sulfuric acid (6.1 M) solution was added to 9 ml of HQ solution in a water (phosphate buffer, pH = 2, $c = 0.2$ M)/ethanol mixture. As expected, the cyclic voltammogram shows a peak related to the oxidation of HQ to *p*-benzoquinone (BQ) (A_1) in the anodic scan, and a peak related to the reduction of BQ to HQ (C_1) in the cathodic scan. When instead of the sulfuric acid solution, 1 ml of diazonium solution containing sulfuric acid (6.1 M) (see experimental section) is added to the HQ solution, there is a large change in the cyclic voltammogram. (Fig. 3, part I, curves b and c). In these voltammograms, a wide range of potentials is scanned to identify all species that are oxidized or reduced. In the anodic scan and in the first cycle (curve b), the voltammogram shows two well-defined anodic peaks at potentials of 0.64 and 1.28 V. These peaks are related to the oxidation of HQ (A_1) and nitrite ion (A_N)⁴⁰ (available in diazonium solution), respectively. In this situation, two weak cathode peaks (C_1 and C_2) can be seen in the reverse cathodic scan at potentials of 0.83 and 0.62 V, respectively. Cathodic peak C_1 is the counterpart of peak A_1 . In the second cycle of the potential sweep (curve c), a new anodic peak (A_2) appears at 0.85 V. This peak is the counterpart of peak C_2 . It should be noted that the same electrochemical behavior observed in the cyclic voltammetry of HQ at different pH values (pH < 8) in the presence of aryldiazonium solution. Since the diazonium solution contains sulfuric acid and changes the pH of the HQ solution, and on the other hand, the HQ/BQ redox system is pH dependent⁴¹, in the experiment conducted in the absence of diazonium ion (Fig. 2, part I, curve a), sulfuric acid (6.1 M) was added to the HQ solution so that the pH of the HQ solution in the absence of diazonium (curve a) became equal to the pH of the HQ solution in the presence of diazonium (curves b and c).

Based on the obtained electrochemical data as well as the spectroscopic data of the product, we propose the following mechanism (Fig. 4, part I) for the oxidation of HQ in the presence of nitrobenzenediazonium sulfate. Accordingly, at the anode surface, HQ loses two electrons and is oxidized to BQ. At the same time, a homolytic dediazonation reaction occurs in the solution^{37,42,43}. As a result of this reaction, aryldiazonium salt (DAZ) is converted into aryl radical (ArR) and dinitrogen molecule.

The reaction between BQ and ArR leads to the formation of intermediate INT, which in the next step by losing an electron becomes the final product, nitro-arylbenzoquinone (ABQ1). According to the proposed mechanism, the anodic (A_2) and cathodic (C_2) peaks are related to the INT/ABQ1 redox couple. It seems that in the absence of reducing agents and metal ions, homolytic dediazonation of diazonium salt is due to its reaction with HQ³⁷. This reaction is shown in Fig. 4, part II.

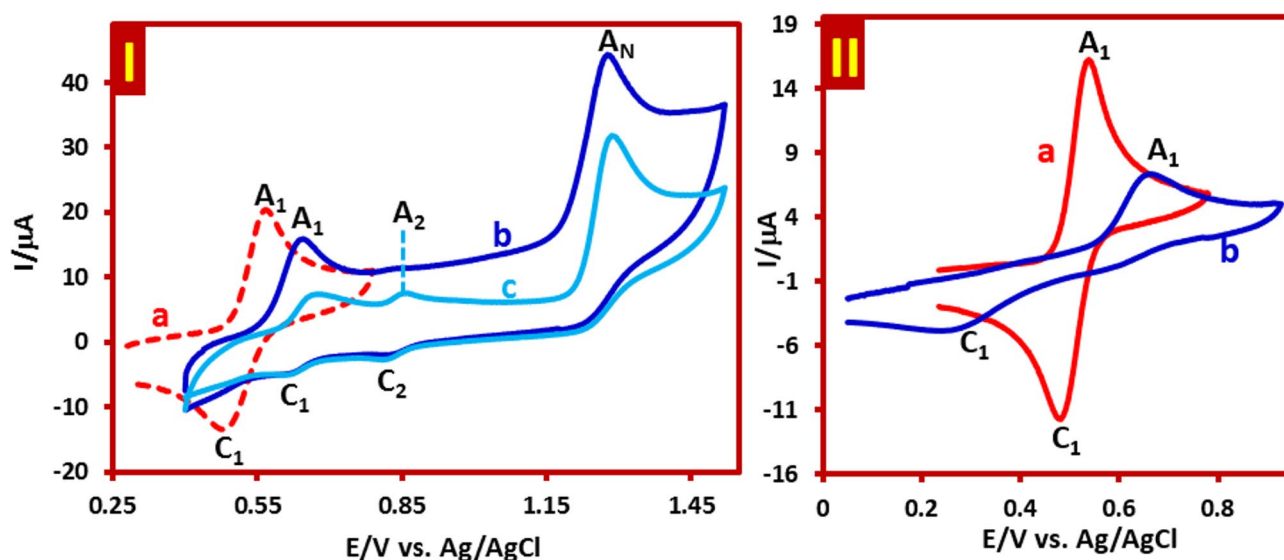


Fig. 3. Part I: Curve a: Cyclic voltammogram of HQ (1 mM) in a water (phosphate buffer, pH = 2, $c = 0.2$ M)/ethanol mixture (50/50 v/v) after addition of 1 mL sulfuric acid (6.1 M). Curves b and c: First and second cycles of cyclic voltammograms of HQ (1 mM) in a water (phosphate buffer, pH = 2, $c = 0.2$ M)/ethanol mixture (50/50 v/v) after addition of 1 mL of prepared diazonium solution (see experimental section). Scan rate: 500 mV/s. Part II: Curve a: Cyclic voltammogram of HQ (1 mM) in a water (bicarbonate buffer, pH 10, $c = 0.2$ M)/ethanol mixture (50/50 v/v) after addition of 1 mL sulfuric acid (6.1 M). Curve b: Cyclic voltammogram of HQ (1 mM) in a water (bicarbonate buffer, pH 10, $c = 0.2$ M)/ethanol mixture (50/50 v/v) after addition of 1 mL of prepared diazonium solution. Scan rate: 100 mV/s. Working electrode: glassy carbon electrode. In all experiments, cells were kept in an ice bath.

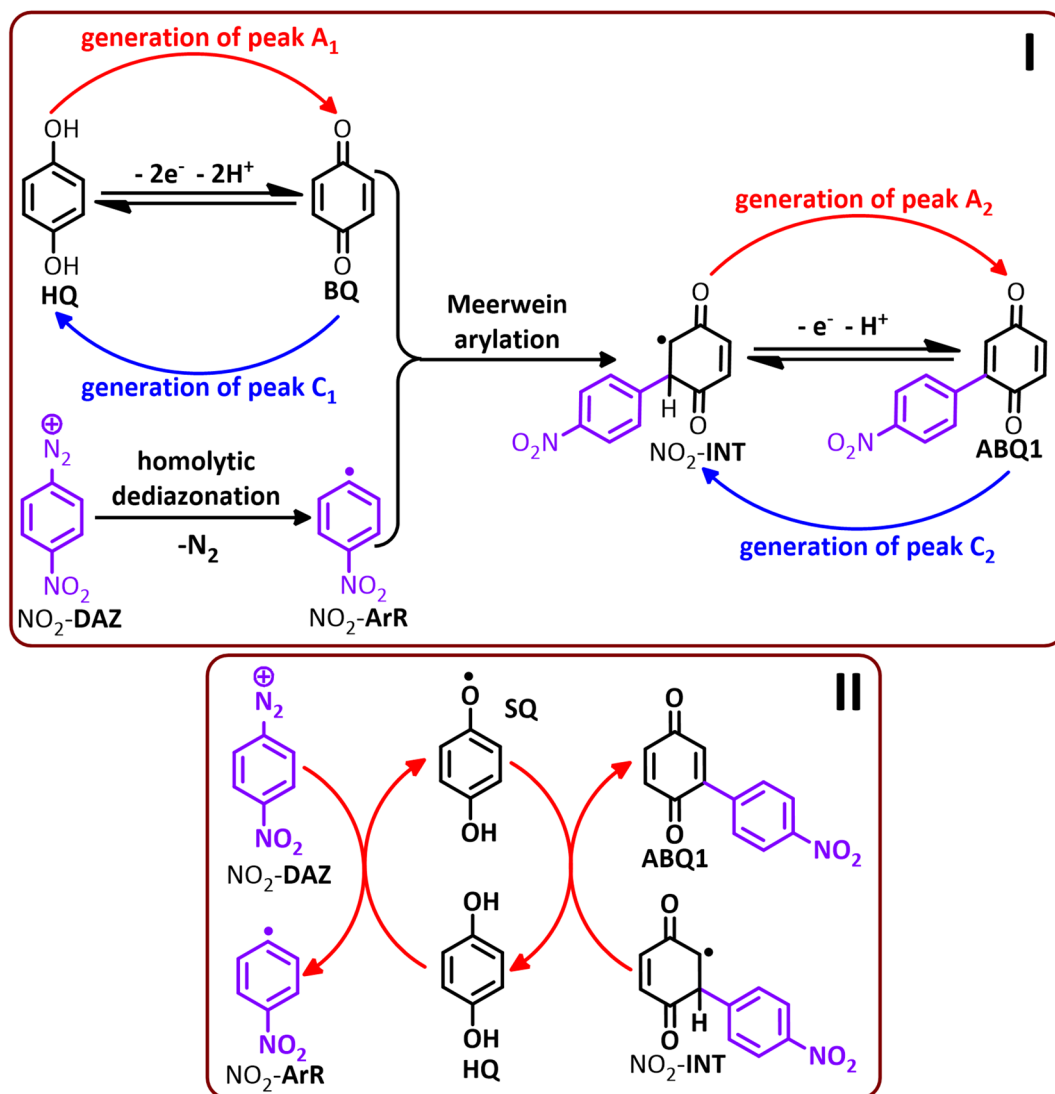


Fig. 4. Electrochemical arylation pathway of hydroquinone and possible homogeneous electron transfer between the species involved in the reaction.

As can be seen, electron transfer between aryldiazonium salt and **HQ** causes the conversion of aryldiazonium salt to aryl radical. On the other hand, as a result of this reaction, **HQ** is converted into semiquinone (**SQ**) by losing an electron. Regarding the oxidation of **INT** and its conversion to the final product (**ABQ1**), two paths seem possible. The first route is the direct oxidation of **INT** on the electrode surface and the second route is its indirect oxidation through the reaction with **SQ**. In contrast to the results obtained in acidic, neutral, and low-alkaline solutions, research conducted at $\text{pH} \geq 10$ suggests that the reaction follows a different course.

Figure 3, part II, curve a, shows the cyclic voltammogram of **HQ** (1 mM) in aqueous (bicarbonate buffer, $\text{pH} 10$, $c = 0.2 \text{ M}$)/ethanol (50/50 v/v) mixture after addition of 1 mL sulfuric acid (6.1 M). The voltammogram recorded under these conditions is similar to the one shown in part I, curve a, except that the peak potentials are shifted towards the negative potentials. When 1 ml of the diazonium solution is added to the **HQ** solution, there is not much change in the cyclic voltammogram. (Fig. 3, part II, curve b) and only its reversibility decreases. This phenomenon may be caused by the fouling of the electrode surface attributed to the immobilization (or adsorption) of the aryl radicals on the surface of the glassy carbon electrode, which reduces the efficiency of the electrode^{44–46}. It seems that as the solution pH increases, the diazonium salt is converted to diazoate and diazohydroxide species, which are much more unstable. Successive hemolytic cleavage of these compounds produces a radical that reacts with the glassy carbon surface⁴⁷.

Since the copper anode has been used in macro-scale electrolysis, it is necessary to slightly modify the proposed mechanism in Fig. 4 for the copper anode. In such conditions, it seems that the oxidation of **HQ** to **BQ** is done through its electron transfer reaction with copper ions (Fig. 5). Also, these ions can oxidize **INT** to **ABQ1**. On the other hand, the formed cuprous ions (Cu^+) can contribute to the reduction of the aryldiazonium salt (**DAZ**) to the aryl radical (**ArR**) (Fig. 5). The use of a copper anode and the catalytic activity of copper ions in the synthesis of aryl-benzoquinones (**ABQ**) is one of the novel and important aspects of this study. The divalent

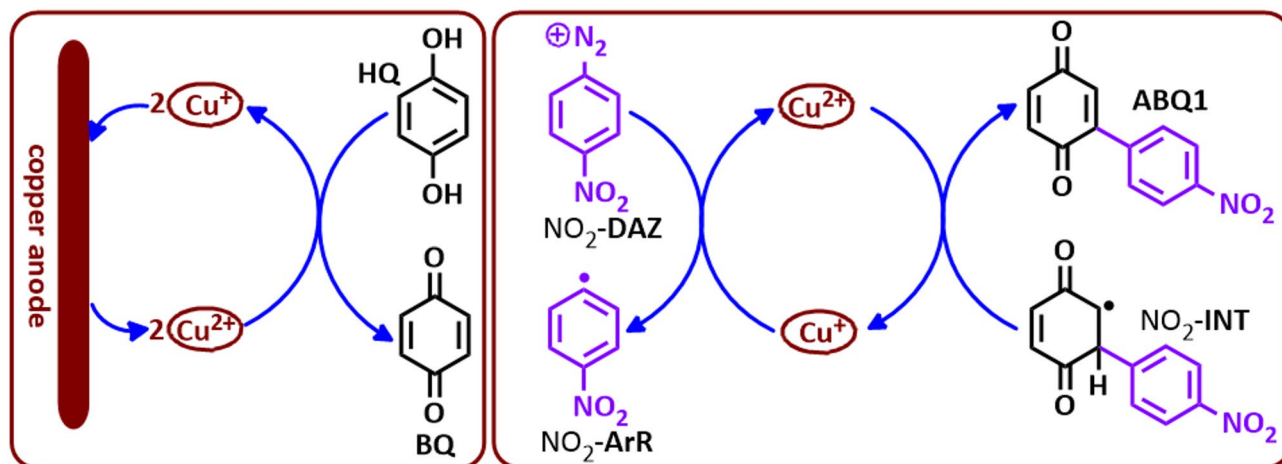


Fig. 5. The possible homogeneous electron transfer between copper ion species and the components involved in the reaction.

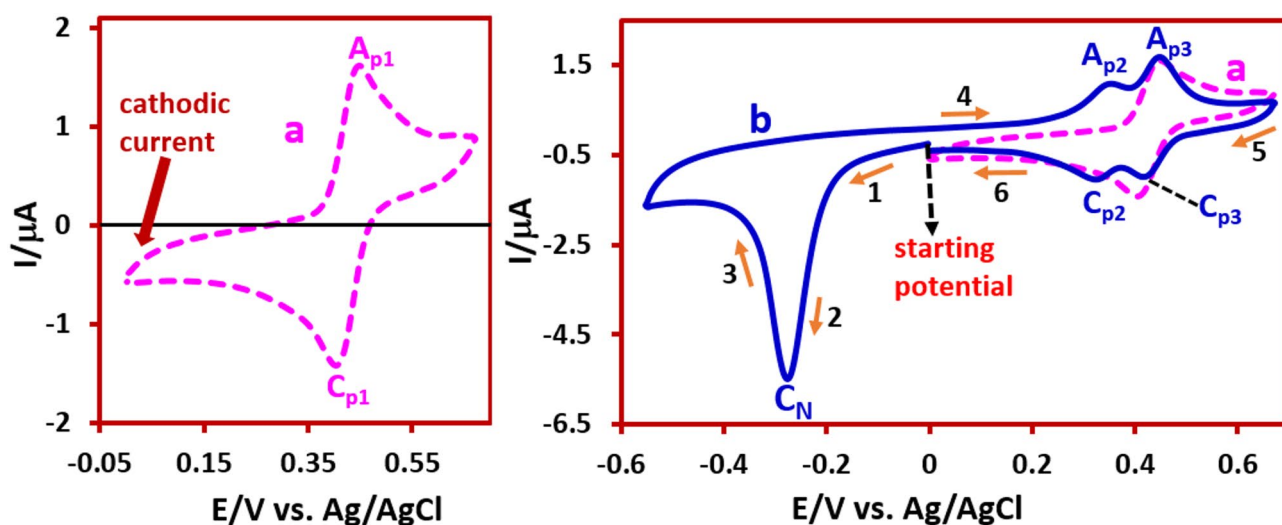


Fig. 6. Cyclic voltammograms of **ABQ1** (1 mM) in a water (phosphate buffer, pH=2, $c=0.2$ M)/ethanol mixture (50/50 v/v) after addition of 1 mL sulfuric acid (6.1 M). (a) Anodic scan has been done first (potential was scanned from +0.0 V to +0.67 V). (b) Cathodic scan has been done first (potential was scanned from 0.0 V to -0.55 V then from -0.55 V to +0.67 V). Scan rate: 25 mV/s. Working electrode: glassy carbon electrode. In all experiments, cells were kept in an ice bath.

copper ions generated from the anodic oxidation can oxidize **HQ** to **BQ**. On the other hand, the monovalent copper ions generated from this reaction can reduce **DAZ** to **ArR** and themselves be oxidized to Cu^{2+} . On the other hand, the Cu^{2+} ions can act as an oxidant to convert **INT** to the final product, **ABQ1**.

The cyclic voltammograms of the product (**ABQ1**) after separation and purification is shown in Fig. 6. In order to further identify the structure of the product and its electrochemical properties, these voltammograms were recorded in two different conditions. In this figure, to record the voltammogram a, first the potential was scanned from 0.0 V towards more positive values (anodic scan), which led to the appearance of a cyclic voltammogram for a Nernstian reversible process. It should be noted that when the starting potential (0 V) is applied, **ABQ1** is reduced to its corresponding nitro-arylhydroquinone (**AHQ1**) at the electrode surface.

The presence of cathodic current at the starting potential (0 V) confirms the reduction of **ABQ1**. Therefore, during potential scanning, the species present on the electrode surface is $\text{NO}_2\text{-AHQ}$. Accordingly, anodic peak A_{p1} is related to the oxidation of $\text{NO}_2\text{-AHQ}$ to **ABQ1**, and cathodic peak C_{p1} is its counterpart and related to the reduction of **ABQ1** to $\text{NO}_2\text{-AHQ}$ (Fig. 7).

In this study, when the cathodic scan is performed first, the shape of the voltammogram changes completely (Fig. 6, curve b). Under these conditions, the cyclic voltammogram shows an irreversible cathodic peak (C_N) and a two reversible redox systems, A_{p2}/C_{p2} and A_{p3}/C_{p3} . As discussed, when the starting potential (0.0 V) is applied, **ABQ1** is reduced to $\text{NO}_2\text{-AHQ}$ at the electrode surface. Therefore, during the cathodic potential scan, peak C_N

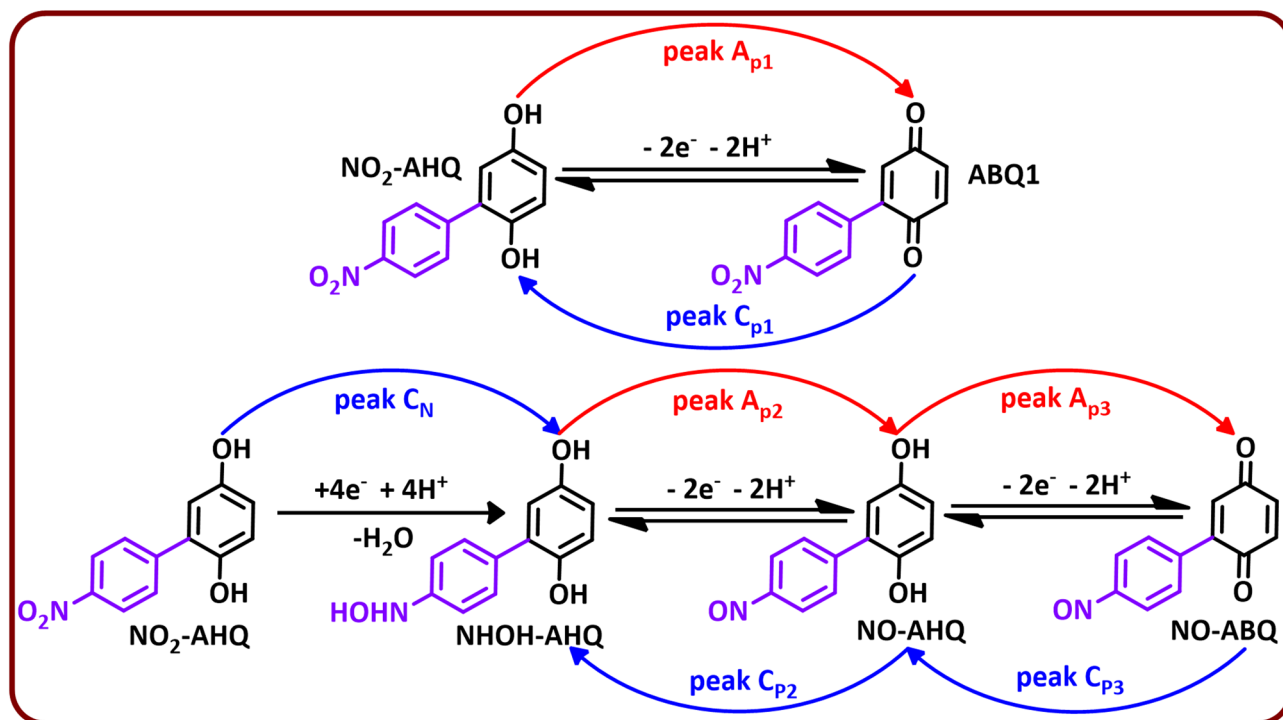


Fig. 7. Electrochemical behavior of ABQ1.

corresponds to the reduction of the nitro group in the $\text{NO}_2\text{-AHQ}$ molecule to the corresponding hydroxylamine (NHOH-AHQ). A_{p2} and C_{p2} peaks are attributed to NHOH-AHQ /nitroso-arylhydroquinone (NO-AHQ) redox couple. Based on this A_{p3} and C_{p3} peaks are attributed to NO-AHQ / NO-ABQ (Fig. 7).

Optimization of reaction conditions

In this part, the effect of factors affecting the yield and purity of the products such as applied current density, amount of electricity, type of electrode and cell and synthesis method has been investigated. The optimization for the synthesis of **ABQ1** was carried out by one-factor-at-a-time (OFAT) approach. The amount of electricity consumption is an important factor in the yield and purity of the product. For the synthesis of **ABQ1**, first the aqueous solution of sodium acetate (0.15 M) (80 ml) containing **HQ** (2 mmol) was electrolyzed in an undivided cell equipped with a copper plate anode and a stainless steel rod cathode under constant current (20 mA) for 10 min. After this period, 1 ml of the produced 4-nitrobenzenediazonium chloride solution is added to the electrochemical cell. The results of studies is shown in Table 1, entries 1–4. The results show that increasing the amount of electricity consumed from 70 to 190 C increases the yield, but a further increase in electricity decreases the yield of **ABQ1** production. Over-oxidation of the product may be the reason for this decrease. Another notable point is that the electricity consumption in these syntheses is lower than the theoretical value, which is due to the oxidation of **HQ** by excess nitrite ions present in the diazonium solution^{48,49} as well as the catalytic activity of copper ions (Fig. 5). The volume of 4-nitrobenzenediazonium chloride solution “added per injection” is another parameter that was optimized, while the total amount of diazonium added was kept constant. Entries 1 and 5–7 show that increasing the sample volume from 0.5 to 3 mL increases production yield. The role of solution pH in the yield of **ABQ1** was also investigated (entries 1 and 8–10). It was found that pH of **HQ** solution has no significant effect on **ABQ1** yield. It seems that increasing the strongly acidic solution containing diazonium salt to the **HQ** solution suppresses the effect of hydroquinone solution pH. Entries 3 and 11–14 show the effect of applied current on **ABQ1** production yield. The results show that the yield of **ABQ1** increases with increasing applied current due to the increased over-potential for **HQ** oxidation and then decreases slightly due to over-oxidation of the product, intermediates or solvent. Furthermore, increasing over-potential increases energy consumption and associated costs.

Again, the effect of the volume of 4-nitrobenzene diazonium chloride solution “added per injection” was investigated when the electricity consumption was 190 coulombs (entries 3 and 15, 16). The role of anode material in the yield of **ABQ1** was also investigated (entries 17–23). It was found that the highest yield is achieved when copper is used as anode.

As mentioned in the previous section and also in Fig. 5, the use of copper anode is one of the innovative aspects of this study due to the catalytic behavior of copper ions. The Cu^{2+} ions can oxidize **HQ** to **BQ**. On the other hand, the generated Cu^+ ions can reduce **DAZ** to **ArR** and themselves be oxidized to Cu^{2+} . On the other hand, Cu^{2+} ions can also convert **INT** to **ABQ1**. Such conditions make it possible to achieve maximum yield when using copper anode. At the end of this section, the cell type was evaluated. For this purpose, a divided cell has been used in optimal conditions (entry 6), and the obtained results indicate a decrease in yield from 71 to

Entry	Electrolysis time (min)	Electricity consumption (C)	Increment time ^a (min)	Sample volume (mL)	Initial pH of hydroquinone solution	Applied current (mA)	Anode material	Yield (%)
1	70	84	3	1	sodium acetate ^b	20	Cu	46.1
2	130	156	6	1	sodium acetate	20	Cu	52.9
3	190	228	9	1	sodium acetate	20	Cu	56.4
4	250	300	12	1	sodium acetate	20	Cu	43.1
5	70	84	1.5	0.5	sodium acetate	20	Cu	38.6
6	70	84	6	2	sodium acetate	20	Cu	71.3
7	70	84	9	3	sodium acetate	20	Cu	71.8
8	70	84	3	1	2	20	Cu	54.1
9	70	84	3	1	5	20	Cu	44.6
10	70	84	3	1	10	20	Cu	51.3
11	190	228	9	1	sodium acetate	5	Cu	46.0
12	190	228	9	1	sodium acetate	10	Cu	47.0
13	190	228	9	1	sodium acetate	15	Cu	57.9
14	190	228	9	1	sodium acetate	25	Cu	55.9
15	190	228	18	2	sodium acetate	20	Cu	71.8
16	190	228	27	3	sodium acetate	20	Cu	51.3
17	130	156	6	2	sodium acetate	20	Zn	37.4
18	130	156	6	2	sodium acetate	20	Al	44.6
19	130	156	6	2	sodium acetate	20	Fe	40.3
20	130	156	6	2	sodium acetate	20	SS ^c	56.3
21	130	156	6	2	sodium acetate	20	Ag	54.4
22	130	156	6	2	sodium acetate	20	graphite	41.2
23	130	156	6	2	sodium acetate	20	Cu	71.3

Table 1. Optimization of effective parameters in **ABQ1** synthesis in batch cell. ^aTime interval between two injections. ^b0.15 M. ^cStainless steel.

54%. Since the direct reduction of diazonium salts at the cathode surface and the formation of aryl radicals is possible⁵⁰, the decrease in yield is a confirmation that the formation of aryl radicals is also performed through direct reduction of diazonium salts at the cathode. Therefore, the use of a divided cell reduces the yield. Based on this result, we propose Fig. 8 for the cathodic generation (direct) of aryl radicals. The proposed mechanism is categorized as convergent paired mechanism in which the intermediates generated at the anode and cathode interact with each other to form the final product⁹.

After optimizing the reaction conditions for the synthesis of **ABQ1**, we investigated the substrate range of different aryldiazoniums and hydroquinones. The results of these studies are shown in Table 2. To this end, we reacted a series of aryldiazonium salts with electron-donating or electron-withdrawing groups at the *para*-position of the benzene ring with hydroquinone as well as 2-methylhydroquinone, leading to the synthesis of the corresponding aryl-benzoquinones in moderate to good yields. Notably, as expected, when unsymmetrical 2-methyl hydroquinone was used, an inseparable mixture of isomers was obtained in moderate yield.

These syntheses have also been performed using a flow cell and the effect of factors affecting the yield and purity of the products such as applied current, flow rate, amount of electricity, and time increment have been investigated. The results of studies is shown in Table 3.

The arrangement of anode and cathode in the flow cell is shown in Fig. 2. Accordingly, the anode is a copper tube and the cathode is a stainless steel rod. As show in Table 3, the best yield, 88.2% (entry 4) is obtained when the applied current is 20 mA, the flow rate is 80 ml/min, the electricity consumption is 72 C, the sample volume of diazonium salt per injection is 2 mL and the injection interval is 6 min.

In another cell design, the shape of the cathode and anode in the flow cell was changed. In this way, a stainless steel tube was used as the cathode and a copper rod as the anode. It should be noted that the dimensions of the tube and rod used in this flow cell are similar to Fig. 2. The synthesis of **ABQ1** with this new cell configuration provides a yield of 52.3%, which is lower than 88.2%.

Conclusion

In this work an eco-friendly electrochemical method was developed for the synthesis of some aryl-benzoquinone derivatives. The synthesis of these compounds was carried out through direct electrolysis of aqueous solution containing hydroquinone in the presence of aryl-diazonium salts in both simple batch and a homemade continuous-flow cells. One of the important points in this work is the easy and cheap preparation of all the equipment needed in both types of cells from common commercial sources. This method is very economical due to the use of electricity instead of chemical reagents and is performed in mild conditions and in water without using toxic solvents and catalysts. In addition, in this work, the electrochemical behavior of hydroquinone in

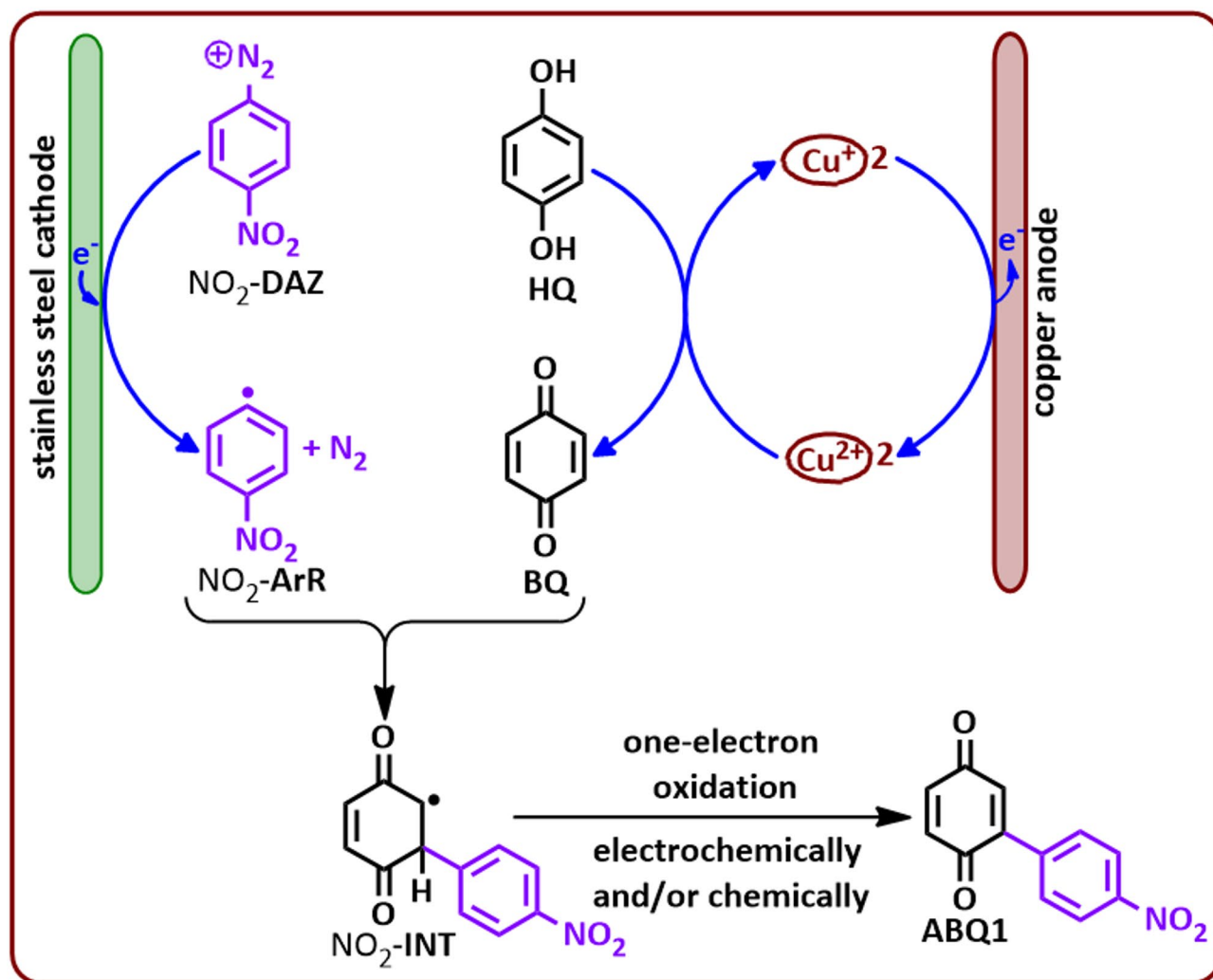
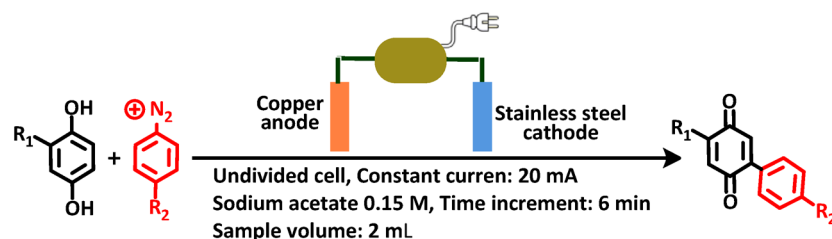


Fig. 8. Direct electrochemical generation of $\text{NO}_2\text{-ArR}$ and formation of ABQ1 .

the presence of aryldiazonium salt was investigated, and based on the results, a detailed mechanism for the electrochemical Meerwein arylation was presented.



Entry	Starting compounds	Electrolysis time.(min)	Product	Name	Yield%
1	R ₁ = -H R ₂ = -NO ₂	70	4'-Nitro-[1,1'-biphenyl]-2,5-dione		ABQ1 71.3
2	R ₁ = -H R ₂ = -H	70	[1,1'-biphenyl]-2,5-dione		ABQ2 70.4
3	R ₁ = -H R ₂ = -OCH ₃	130	4'-Methoxy-[1,1'-biphenyl]-2,5-dione		ABQ3 86.4
4	R ₁ = -H R ₂ = -Cl	70	4'-Chloro-[1,1'-biphenyl]-2,5-dione		ABQ4 51.3
5	R ₁ = -H R ₂ = -Br	70	4'-Bromo-[1,1'-biphenyl]-2,5-dione		ABQ5 39.1
6	R ₁ = -H R ₂ = -I	70	4'-Iodo-[1,1'-biphenyl]-2,5-dione		ABQ6 80.4
7	R ₁ = -H R ₂ = -F	70	4'-Fluoro-[1,1'-biphenyl]-2,5-dione		ABQ7 72.8
8	R ₁ = -CH ₃ R ₂ = -NO ₂	70	4-Methyl (and 3-methyl) -4'-nitro-[1,1'-biphenyl]-2,5-dione isomers ratio%: 58.9/41.1 ^a		ABQ8 66.7
9	R ₁ = -CH ₃ R ₂ = -Cl	70	4'-Chloro-4-methyl (and 3-methyl) -[1,1'-biphenyl]-2,5-dione isomers ratio%: 50.4/49.6		ABQ9 43.3
10	R ₁ = -CH ₃ R ₂ = -Br	130	4'-Bromo-4-methyl (and 3-methyl) -[1,1'-biphenyl]-2,5-dione isomers ratio%: 50.4/49.6		ABQ10 38.4
11	R ₁ = -CH ₃ R ₂ = -I	70	4'-Iodo-4-methyl (and 3-methyl) -[1,1'-biphenyl]-2,5-dione isomers ratio%: 49.8/50.2		ABQ11 62.3

Table 2. Scope of the synthesis of aryl-benzoquinone derivatives (ABQ).

^aThe ratio of the isomers was calculated from ¹H NMR spectrum using the signals intensity of methyl group..

Entry	Electrolysis time (min)	Electricity consumption (C)	Increment time (min) ^a	Sample volume (mL)	Flow rate (mL/min)	Applied current (mA)	Yield (%)
1	60	72	3	1	80	20	66.7
2	120	144	6	1	40	20	33.4
3	180	216	9	1	26.6	20	26.8
4	60	72	6	2	80	20	88.2
5	60	72	9	3	80	20	47.0
6	120	144	12	2	40	20	40.8
7	120	144	18	3	40	20	33.3
8	60	36	6	2	80	10	42.5
9	60	108	6	2	80	30	57.4

Table 3. Optimization of effective parameters in ABQ1 synthesis in flow cell. ^aTime interval between two injections.

Data availability

The datasets used and/or analyzed during the current study available from the corresponding author on request.

Received: 26 February 2025; Accepted: 13 May 2025

Published online: 17 May 2025

References

- Waldvogel, S. R., Lips, S., Selt, M., Riehl, B. & Kampf, C. J. Electrochemical arylation reaction. *Chem. Rev.* **118**, 6706–6765 (2018).
- Nematollahi, D., Mohamadighader, N., Roshani, M., Hashemi-Mashouf, M. M. & Goudarztalejerdi, A. Successive paired electrochemical synthesis as a green strategy for late-stage modification of flutamide an anti-cancer drug. Gram-scale synthesis and antibacterial activity. *Electrochem. Acta* **502**, 144741 (2024).
- Martins, G. M., Zimmer, G. C., Mendes, S. R. & Ahmed, N. Electrifying green synthesis: recent advances in electrochemical annulation reactions. *Green Chem.* **22**, 4849–4870 (2020).
- Martins, G. M., Shirinfar, B., Hardwick, T., Murtaza, A. & Ahmed, N. Organic electrosynthesis: electrochemical alkyne functionalization. *Catal. Sci. Technol.* **9**, 5868–5881 (2019).
- Sbei, N., Hardwick, T. & Ahmed, N. Green chemistry: Electrochemical organic transformations via paired electrolysis. *ACS Sustain. Chem. Eng.* **9**, 6148–6169 (2021).
- Talebi, M. R. & Nematollahi, D. Electrochemical synthesis of sulfonamide derivatives: Electrosynthesis conditions and reaction pathways. *ChemElectroChem* **11**, e202300728 (2024).
- Ibanez, J. G., Frontana-Urbe, B. A. & Vasquez-Medrano, R. Paired electrochemical processes: Overview, systematization, selection criteria, design strategies, and projection. *J. Mex. Chem. Soc.* **60**, 247–260 (2016).
- Frontana-Urbe, B. A., Little, R. D., Ibanez, J. G., Palma, A. & Vasquez-Medrano, R. Organic electrosynthesis: A promising green methodology in organic chemistry. *Green Chem.* **12**, 2099–2119 (2010).
- Nematollahi, D., Alizadeh, S., Amani, A. & Khazalpour, S. *Practical Aspects of Electroorganic Synthesis* (Elsevier, 2024).
- Nematollahi, D. & Varmaghani, F. Paired electrochemical synthesis of new organosulfone derivatives. *Electrochim. Acta* **53**, 3350–3355 (2008).
- Sun, J. et al. Sulfonyl hydrazides as a general redox-neutral platform for radical cross-coupling. *Science* <https://doi.org/10.1126/science.adu6406> (2025).
- Sun, J., Wang, S., Harper, K. C., Kawamata, Y. & Baran, P. S. Stereoselective amino alcohol synthesis via chemoselective electrocatalytic radical cross-couplings. *Nat. Chem.* **17**, 44–53 (2025).
- Ewing, T. E. et al. Pyrolytic carbon: An inexpensive, robust, and versatile electrode for synthetic organic electrochemistry. *Angew. Chem. Int. Ed.* **64**, e202417122 (2025).
- Jafarzadeh, M. et al. Electrifying P (V): Access to polar and radical reactivity. *Angew. Chem. Int. Ed.* **64**, e202421163 (2025).
- Dandawate, P. R., Vyas, A. C., Padhye, S. B., Singh, M. W. & Baruah, J. B. Perspectives on medicinal properties of benzoquinone compounds. *Mini-Rev. Med. Chem.* **10**, 436–454 (2010).
- Silakari, P. & Piplani, P. *p*-Benzoquinone as a privileged scaffold of pharmacological significance: A review. *Mini-Rev. Med. Chem.* **20**, 1586–1609 (2020).
- Foland, L. D. et al. Rearrangement of 4-alkynylcyclobutenones. A new synthesis of 1,4-benzoquinones. *J. Am. Chem. Soc.* **111**, 975–989 (1989).
- Abreu, B. L., Bouffroua, H., Moore, J. C., Poliakov, M. & George, M. W. Telescoped continuous flow synthesis of 2-substituted 1,4-benzoquinones via oxidative dearomatization of *para*-substituted phenols using singlet oxygen in supercritical CO₂. *Synthesis* **54**, 3651–3657 (2022).
- Saa, J. M., Llobera, A., Garcia-Raso, A., Costa, A. & Deya, P. M. Metalation of phenols. Synthesis of benzoquinones by the oxidative degradation approach. *J. Org. Chem.* **53**, 4263–4273 (1988).
- Mathur, P., Avasare, V. D. & Mobin, S. M. Iron pentacarbonyl assisted photochemical route to 2, 5-and 2,6-divinyl-substituted 1,4-benzoquinones from 1-ene-3-yne. *Tetrahedron* **64**, 8943–8946 (2008).
- Kim, S., Matsubara, R. & Hayashi, M. Activated carbon-promoted dehydrogenation of hydroquinones to benzoquinones, naphthoquinones, and anthraquinones under molecular oxygen atmosphere. *J. Org. Chem.* **84**, 2997–3003 (2019).
- Sprang, F., Herszman, J. D. & Waldvogel, S. R. Electrochemical oxidation of phenols in flow: A versatile and scalable access to *para*-benzoquinones. *Green Chem.* **24**, 5116–5124 (2022).
- Nematollahi, D., Momeni, S. & Khazalpour, S. Different strategies in electrochemical synthesis of new mono and di-substituted hydroquinone and benzoquinone. *Electrochim. Acta* **147**, 310–318 (2014).
- Nematollahi, D. & Hesari, M. Electrochemical synthesis of amino-substituted 1,2-benzoquinone derivatives. *J. Electroanal. Chem.* **577**, 197–203 (2005).
- Shanmugam, V. et al. Electrochemical synthesis of quinones and other derivatives in biphasic medium. *Tetrahedron Lett.* **58**, 2294–2297 (2017).
- Zhang, L. et al. Direct electrochemical synthesis of quinones from simple aromatics and heteroaromatics. *Chem. Commun.* **59**, 7255–7258 (2023).

27. Sprang, F., Klein, J. & Waldvogel, S. R. Direct anodic conversion of 4-hydroxybenzaldehydes into benzoquinones. *ACS Sustain. Chem. Eng.* **11**, 7755–7764 (2023).
28. Meerwein, H., Büchner, E. & van Emster, K. Über die einwirkung aromatischer diazoverbindungen auf α , β -ungesättigte carbonylverbindungen. *J. Prakt. Chem.* **152**, 237–266 (1939).
29. Kindt, S. & Heinrich, M. R. Recent advances in Meerwein arylation chemistry. *Synthesis* **48**, 1597–1606 (2016).
30. Pokhodylo, N. T. Recent advances in the application of Meerwein arylation for the synthesis of complex heterocycles at the Ivan Franko National University of Lviv (microreview). *Chem. Heterocycl. Compd.* **59**, 406–408 (2023).
31. Ghosh, I., Marzo, L., Das, A., Shaikh, R. & König, B. Visible light mediated photoredox catalytic arylation reactions. *Acc. Chem. Res.* **49**, 1566–1577 (2016).
32. Diesendorf, N. & Heinrich, M. R. Current advances in Meerwein-type radical alkene functionalizations. *Synthesis* **54**, 1951–1963 (2022).
33. Lide, D. R. *CRC handbook of chemistry and physics* Vol. 85 (CRC Press, 2004).
34. Kvalnes, D. An optical method for the study of reversible organic oxidation—reduction systems. IV. Arylquinones. *J. Am. Chem. Soc.* **56**, 2478–2481 (1934).
35. Zhang, S., Song, F., Zhao, D. & You, J. Tandem oxidation—oxidative C-H/C-H cross-coupling: Synthesis of arylquinones from hydroquinones. *Chem. Commun.* **49**, 4558–4560 (2013).
36. Walker, S. E., Jordan-Hore, J. A., Johnson, D. G., Macgregor, S. A. & Lee, A. L. Palladium-catalyzed direct C-H functionalization of benzoquinone. *Angew. Chem.* **126**, 14096–14099 (2014).
37. Honraedt, A., Le Callonnec, F., Le Grogne, E., Fernandez, V. & Felpin, F. X. C-H arylation of benzoquinone in water through aniline activation: Synergistic effect of graphite-supported copper oxide nanoparticles. *J. Org. Chem.* **78**, 4604–4609 (2013).
38. Yang, B., Yao, W., Xia, X. F. & Wang, D. Mn-Catalyzed 1,6-conjugate addition/aromatization of *para*-quinone methides. *Org. Biomol. Chem.* **16**, 4547–4557 (2018).
39. Wang, D., Ge, B., Li, L., Shan, J. & Ding, Y. Transition metal-free direct C-H functionalization of quinones and naphthoquinones with diaryliodonium salts: Synthesis of aryl naphthoquinones as β -secretase inhibitors. *J. Org. Chem.* **79**, 8607–8613 (2014).
40. Salahifar, E., Nematollahi, D., Mahyari, A. & Nosratzadegan, K. A green and safe galvanostatic method for the synthesis of 4-nitrocatechol in aqueous solution. *J. Electrochem. Soc.* **162**, G19–G24 (2015).
41. Beiginejad, H., Nematollahi, D., Bayat, M., Varmaghani, F. & Nazaripour, A. Experimental and theoretical analysis of the electrochemical oxidation of catechol and hydroquinone derivatives in the presence of various nucleophiles. *J. Electrochem. Soc.* **160**, H693–H698 (2013).
42. Chehimi, M. M., Pinson, J. & Mousli, F. *Aryl Diazonium Salts and Related Compounds: Surface Chemistry and Applications* (Springer, 2022).
43. Wang, Y., Zhu, S. & Zou, L. H. Recent advances in direct functionalization of quinones. *Eur. J. Org. Chem.* **2019**, 2179–2201 (2019).
44. Kullapere, M., Mirkhalaf, F. & Tammeveski, K. Electrochemical behaviour of glassy carbon electrodes modified with aryl groups. *Electrochim. Acta* **56**, 166–173 (2010).
45. Vase, K. H., Holm, A. H., Norrman, K., Pedersen, S. U. & Daasbjerg, K. Covalent grafting of glassy carbon electrodes with diaryliodonium salts: New aspects. *Langmuir* **23**, 3786–3793 (2007).
46. Koefoed, L., Pedersen, S. U. & Daasbjerg, K. Covalent modification of glassy carbon surfaces by electrochemical grafting of aryl iodides. *Langmuir* **33**, 3217–3222 (2017).
47. Hetemi, D., Noël, V. & Pinson, J. Grafting of diazonium salts on surfaces: Application to biosensors. *Biosensors* **10**, 4 (2020).
48. John, P. B. The kinetics and mechanism of oxidation of hydroquinone and chlorohydroquinone in the presence of nitrous acid in aqueous acid solution. *J. Chem. Soc. Perkin Trans 2* 957–60 (1994).
49. Khalafi, L. & Rafiee, M. Kinetic study of the oxidation and nitration of catechols in the presence of nitrous acid ionization equilibria. *J. Hazard. Mater.* **174**, 801–806 (2010).
50. Zeng, X. The strategies towards electrochemical generation of aryl radicals. *Chem. Eur. J.* **30**, e202402220 (2024).

Acknowledgements

The authors acknowledge the Bu-Ali Sina University Research Council and Center of Excellence in Development of Environmentally Friendly Methods for Chemical Synthesis (CEDEFMCS) for their support of this work.

Author contributions

D.N. supervision, project administration, resources, writing-review & editing. A.S. Project administration. M.M. investigation, writing-original draft. S.S. investigation.

Declarations

Competing interests

The authors declare no competing interests.

Additional information

Supplementary Information The online version contains supplementary material available at <https://doi.org/10.1038/s41598-025-02504-y>.

Correspondence and requests for materials should be addressed to D.N.

Reprints and permissions information is available at www.nature.com/reprints.

Publisher's note Springer Nature remains neutral with regard to jurisdictional claims in published maps and institutional affiliations.

Open Access This article is licensed under a Creative Commons Attribution-NonCommercial-NoDerivatives 4.0 International License, which permits any non-commercial use, sharing, distribution and reproduction in any medium or format, as long as you give appropriate credit to the original author(s) and the source, provide a link to the Creative Commons licence, and indicate if you modified the licensed material. You do not have permission under this licence to share adapted material derived from this article or parts of it. The images or other third party material in this article are included in the article's Creative Commons licence, unless indicated otherwise in a credit line to the material. If material is not included in the article's Creative Commons licence and your intended use is not permitted by statutory regulation or exceeds the permitted use, you will need to obtain permission directly from the copyright holder. To view a copy of this licence, visit <http://creativecommons.org/licenses/by-nc-nd/4.0/>.

© The Author(s) 2025